

Mechanical behavior of steel-concrete composite decks with perfobond shear connectors

Hamed Allahyari^a, Mehdi Dehestani^{*}, Morteza H.A. Beygi^b,
Bahram Navayi Neyfa^c and Ebrahim Rahmani^d

Faculty of Civil Engineering, Babol Noshirvani University of Technology, Babol, Iran

(Received September 31, 2013, Revised March 09, 2014, Accepted March 23, 2014)

Abstract. Exodermic deck systems are new composite steel grid deck systems which have been used in various projects during the past decade. One of the eminent features of this system is considerable reduction in the structure weight compared to the ordinary reinforced concrete decks and also reduction in construction time by using precast Exodermic decks. In this study, dynamic properties of the Exodermic deck bridges with alternative perfobond shear connectors are investigated experimentally. In order to evaluate the dynamic properties of the decks, peak picking and Nyquist circle fit methods are employed. Frequencies obtained experimentally are in good agreement with the results of the finite-element solution, and the experimental results show that the first mode is the most effective mode among the obtained modes. The first four modes are the rigid translational motion modes, and the next two modes seem to be rigid rotational motion modes around a horizontal axis. From the 7th mode onwards, modes are flexible. The range of damping ratios is about 0.5%. Furthermore, the static behavior of the Exodermic decks under a static load applied at the center of the decks was investigated. Failure of the decks under positive bending was punching-shear. The bending strength of the decks under negative bending was about 50 percent of their strength under positive bending. In addition, the weight of an Exodermic deck is about 40% of that of an equivalent reinforced concrete slab.

Keywords: exodermic decks; shear connector; dynamic properties; composite structure

1. Introduction

Regarding the increasing demands for rapid construction of bridges with lower dead loads and costs, various types of structural systems have been proposed for bridge decks. Due to the high tensile strength of steel and the remarkable compression strength of concrete at lower cost, steel-concrete composites are the most common composites used in the construction.

A convenient performance for the steel-concrete composite structures can be achieved,

*Corresponding author, Assistant Professor, E-mail: dehestani@gmail.com

^a Graduate Student, E-mail: allahyari.h@gmail.com

^b Assistant Professor, E-mail: m.beygi@nit.ac.ir

^c Associate Professor, E-mail: navayi@nit.ac.ir

^d Graduate Student, E-mail: ebrahim.rahmani@stu.nit.ac.ir

provided the relative displacement of concrete and steel sections at their interface be prevented or at least be reduced. Chemical adhesions or bonds, interface friction and mechanical interlocking do not provide sufficient resistance to heavy shear forces. Hence, to assure the shear transfer, various types of mechanical connectors between steel and concrete such as channels, reinforcing steel, headed shear studs and welded structural steel elements have been considered. The headed shear studs are the most widely used connectors in steel-concrete composite structures.

Nishimura *et al.* (1971) proposed to connect steel girder with concrete slab by means of horizontal bars bearing on ribs welded on the upper flange. This sort of connection led to a novel steel-concrete composite deck system called Exodermic deck in which the perfobond strip shear connector is used. The main advantages of these shear connectors are high shear resistance and suitable performance in fatigue (The D.S Brown Company 2007). The perfobond rib shear connectors were first developed by Leonhardt *et al.* (1987).

Zellner (1987) introduced a perfobond rib shear connector consisting of a perforated steel plate that is welded to the steel beam upper flange in a composite deck slab. A comparative experimental study by Oguejiofor and Hosain (1992) on headed stud shear connectors and perfobond rib shear connectors revealed that the perfobond rib connector is a viable alternative to the headed studs. In a subsequent study by Oguejiofor and Hosain (1994) the influences of a number of parameters on the shear capacity of the perfobond rib connection were investigated and eventually an expression for computing the shear capacity of perfobond rib connectors was proposed. Velandá and Hosain (1992) conducted an experimental study on the feasibility of using perfobond rib type shear connectors in composite beams. The results of 48 push-out test specimens in their study were used in a numerical verifying study by Oguejiofor and Hosain (1996) using the finite element analysis.

Higgins and Mitchell (2001) conducted a comprehensive experimental study on the behavior of composite bridge decks with perfobond rib shear connectors. The full-scale tests of prototype bridge decks with perfobond shear in their study included both static and fatigue loading. The push out tests on connector resistance of concrete deck plates with precast concrete slab were conducted by Macháček and Studnicka (2002).

Ciutina and Stratan (2008) studied the performances of shear connectors under cyclic and monotonic loading, through push out and respectively push-pull tests and investigated the effective parameters such as resistance, ductility and stiffness.

Kim and Jeong (2009) studied the behavior of a steel-concrete deck slab system with profiled steel sheeting and perfobond rib shear connectors via experimental tests and numerical modeling. They reported eventually that the ultimate load-carrying capacity of the composite deck system is at least 220% greater than that of the reinforced concrete (RC) deck system and also the deck weighs about 23% less than the RC deck system.

In a subsequent study by Kim and Jeong (2010) the ultimate behavior of the steel-concrete deck slab system was experimentally investigated, and the experimental results demonstrated that the ultimate strength of the deck system under hogging bending action are approximately 2.5 and 7.1 times greater than those of an RC deck, respectively, while the deck weighs about 25% less than RC deck systems.

The shear strength of the shear connection of the unfilled composite steel grid bridge deck was evaluated by Kim and Choi (2010). They employed 14 push-out tests to determine the shear strength and slip characteristics of the connection.

Bending behavior of steel-concrete composite beam was investigated by Gorkem and Husem (2013). Results disclosed declining load bearing and deflection capacities of composite beams

with increasing encasement depths into concrete. The dynamic behaviors of a simply-supported steel-concrete composite beam were studied by Hou *et al.* (2012), and finally were compared with the theoretical results.

Although many research works have been accomplished on composite structures with perfobond shear connectors, the experimental dynamic properties of these composite structures have been rarely investigated. In this study, Exodermic steel-concrete composite deck specimens with perfobond shear connectors are constructed and the mechanical behavior of the decks under static loading are investigated. Also, in order to achieve the dynamic properties of the Exodermic decks, natural frequencies, damping ratios as well as some physical properties such as the stiffness and the modal mass are obtained using the frequency response function (FRF) method.

2. Materials

In order to investigate the mechanical behavior of steel-concrete composite decks with perfobond shear connectors, three Exodermic decks, as shown in Fig. 1, with 100 cm of length and 90 cm of width were constructed. The composite decks consist of steel and concrete parts.

A set of IPE 160 steel sections' webs which is type of ST37 with 2400 kg/m^3 of yield stress was cut off to provide T-shaped steel sections. Circular holes with 19 mm of diameter and 51 mm spacing were punched on the web of the T-shaped steel sections. The webs of the T-shaped steel sections were also punched by milling machine to produce bean-shaped holes with dimensions of $25 \times 8 \text{ mm}$ and 102 mm spacing. Details of the holes punched on the main bars (T-shaped steel sections) are shown in Fig. 2.

As shown in Fig. 3, the spacing between the main bars is 33 cm and the rectangular distribution bars with $6 \times 25 \text{ mm}$ of section dimensions and 90 cm of length were passed through the bean-shaped holes and they were welded to the main bars (Fig. 4).

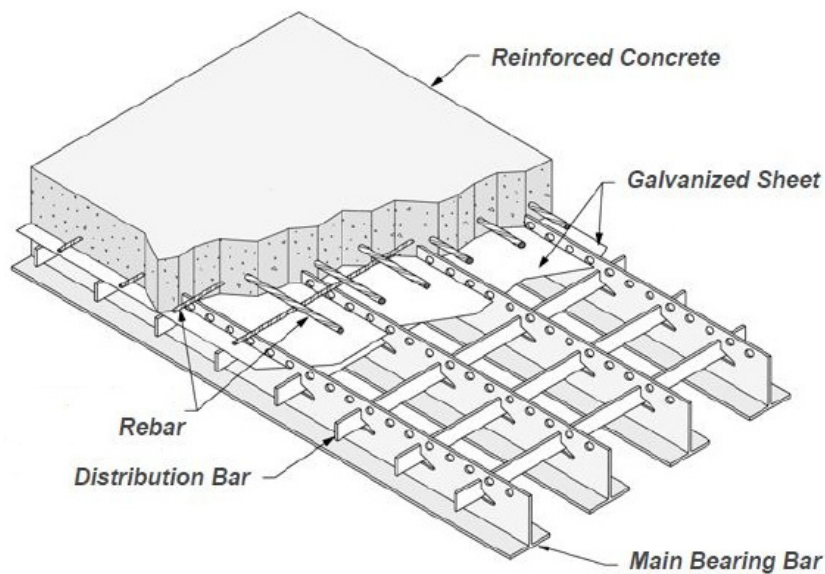


Fig. 1 An exodermic bridge deck with perfobond shear connectors (The D.S Brown Company (2007))

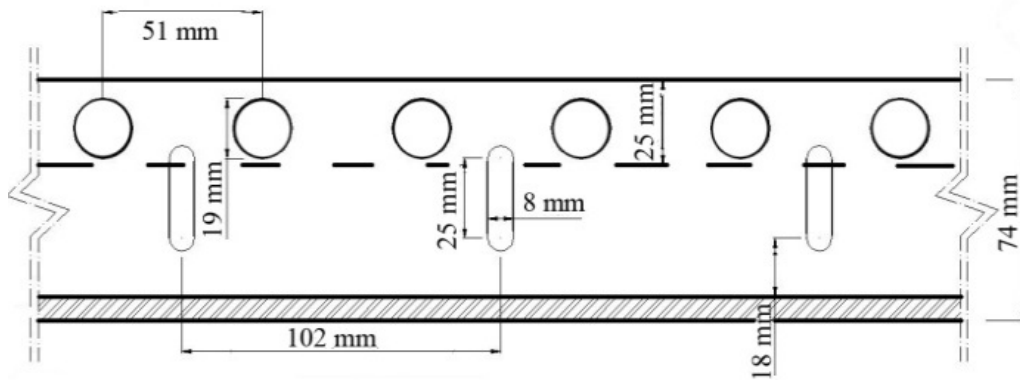


Fig. 2 Details of the holes punched on the main bars



Fig. 3 An assembled steel grid

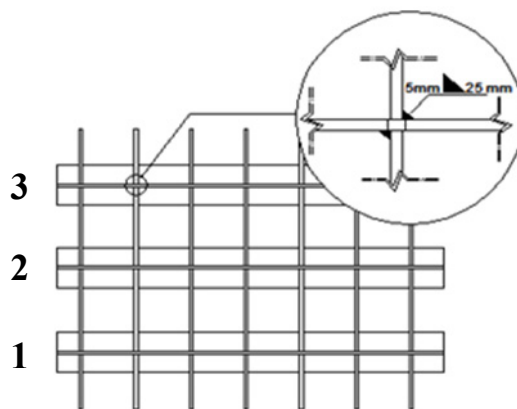


Fig. 4 Welding distribution bars to the main bars details



Fig. 5 An Exodermic deck prepared to concrete casting

Natural fine and natural coarse aggregates with maximum size of 12.5 mm (based on ASTM C33 (2001)) were used in concrete mixtures. Bulk specific gravities of coarse and fine aggregates were 2.7, and their water absorptions were 2.5% and 3%, respectively. The fineness modulus of fine aggregates was 2.82. Sieve analysis was conducted for coarse and fine aggregates based on ASTM C33 (2001), and the results are given in Table 1.

Portland cement conforming to ASTM C150 Type II (modified cement) with density of 3150 Kg/m³ and specific area of 0.306 m²/gr was used in the mixtures. Chemical compounds of the cement are listed in Table 2.

Table 1 Sieve analysis for aggregates

A. Coarse aggregate			
Sieve No.	Sieve size (mm)	Percentage passing (%)	ASTM limits (%)
1/2	12.5	100	90-100
3/8	9.5	42.63	40-70
4	4.75	0.86	0-15
8	2.63	-	0-5
B. Fine aggregate			
Sieve No.	Sieve size (mm)	Percentage passing (%)	ASTM limits (%)
4	4.75	100	100
8	2.63	81.98	80-100
16	1.18	63.66	50-85
30	0.60	45.15	25-60
50	0.30	23.31	9-30
100	0.15	4.12	2-10

Table 2 Cement composition

Compound	Percent (%)	Compound	Percent (%)
SiO ₂	21.25	CaO	64.07
Al ₂ O ₃	4.95	MgO	1.20
Fe ₂ O ₃	3.19	SO ₃	2.04
K ₂ O	0.63	Na ₂ O	0.38

Table 3 Mix proportion (kg/m³)

Dry density (kg/m ³)	Fine aggregate (kg)	Coarse aggregate (kg)	Cement (kg)	Water (kg)	Percent (%)
2400	760	940	450	211	64.07

Details of the concrete mixtures proportioning are given in Table 3. A laboratory concrete mixer was used to mix the concrete mixtures for five minutes. In order to assure a convenient shear transfer in connectors, the fresh concrete should have sufficient workability to cross the punched holes on the main bars. Eventually, the fresh concrete with slump of 80 mm was casted on the steel part of the composite deck.

The average compressive strength of the 10 cm-cube specimens at the time of testing (60 days) was evaluated 57.38 MPa, and the elasticity modulus of standard cylinders (100 × 150 cm) was obtained 294.17 GPa.

3. Dynamic evaluation

Modal testing is an experimental technique to obtain the modal model of a linear vibrational system. This technique is based on the relationship between vibration response of a point of the structure which is excited at the same point or another point in form of a function depending on excited frequency. For exciting force $f(t) = F(\omega)e^{j\omega t}$, where t and ω are time and circular frequency and j is equal to $\sqrt{-1}$, the system response is expressed by $x(t) = X(\omega)e^{j\omega t}$ where the amplitude of the response $X(\omega)$ could be a complex function. The substitution of these values into the equation of motion yields (He and Fu 2001)

$$\frac{X(\omega)}{F(\omega)} = \frac{1}{k - \omega^2 m + j\omega c} \quad (1)$$

Where k , m and c are stiffness, modal mass and damping coefficient, respectively. The ratio given by Eq. (1) which is usually expressed by $\alpha(\omega)$ is known as Frequency Response Function (FRF) which is the most important function used in modal analysis. Although FRF is expressed by the proportion of the response to the force, it is independent from both of the force and the response. Other kinds of response such as velocity or acceleration response can be used instead of displacement response in Eq. (1) and thus various FRF's can be obtained in modal analysis. If FRF was obtained by using displacement response data, it would be called "Receptance", if it was obtained by using velocity response data, it would be called "Mobility" and if it was obtained by

using acceleration response data, it would be called “Accelerance”. Choosing convenient type of the FRF leads to obtain desired characteristic explicitly. The common methods for the graphical presentation of an FRF are the linear or Logarithmic amplitude-frequency graph, Nyquist plot, etc. (He and Fu 2001).

3.1 FRF plot

A distinct feature of the linear-linear plot of an FRF is the prominence of the resonance. Due to this, it is difficult to appreciate the whole FRF curve. In order to overcome this problem, the magnitude of the FRF is converted into its decibel (dB) scale (He and Fu 2001), which was considered in this research.

3.2 Peak picking

One of the simplest methods to estimate damping ratio and natural frequency by the FRF plot is the peak picking method. Based on this method, the frequency of resonance point (the peak value of the FRF plot) is a natural frequency ω_r of structure. If two points were picked in opposite sides of the resonance point with 3 dB of amplitude on the FRF plot, the relationship between the frequencies and the damping ratio could be expressed by Eq. (2) (He and Fu 2001).

$$\zeta = \frac{\omega_2 - \omega_1}{2\omega_r} \tag{2}$$

Where ω_i ($i = 1,2$) and ζ are frequencies and damping ratio, respectively. One of the defects of the peak picking method is related to the recorded data with low density or the case that FRF data has noise. The accuracy of this method decreases in these cases.

3.3 Nyquist plot

Nyquist plot presents the real part of the FRF against its imaginary part on the complex plane. The advantage of using Nyquist plot comes from the circularity on the complex plane. However, all of the Nyquist plots of receptance, mobility and accelerance FRFs seem circular, only the Nyquist for mobility FRF (for structural damping) is the real one. For a single degree of freedom (SDoF) system with viscous damping, mobility FRF is expressed by Eq. (3) (He and Fu 2001).

$$Y(\omega) = \frac{j\omega}{k - m\omega^2 + j\omega c} \tag{3}$$

The real and the imaginary parts of Eq. (3) are

$$\text{Re}[Y(\omega)] = \frac{\omega^2 c}{(k - m\omega^2)^2 + (\omega c)^2} \tag{4}$$

$$\text{Im}[Y(\omega)] = \frac{\omega(k - m\omega^2)}{(k - m\omega^2)^2 + (\omega c)^2} \tag{5}$$

Therefore the mathematical relation can be found easily (He and Fu 2001).

$$\left(\operatorname{Re} \left[Y(\omega) - \frac{1}{2c} \right] \right)^2 + (\operatorname{Im}[Y(\omega)])^2 = \left(\frac{1}{2c} \right)^2 \quad (6)$$

Expressed equation is a circle with radius of $1/2c$. Theoretically, it is possible to demonstrate that the natural frequency occur in a place which has the maximum variation rate of the arc length on the Nyquist plot. By dividing the imaginary value of a point near to the natural frequency's place on the Nyquist plot by its real value, the damping ratio is expressed by Eq. (7) (He and Fu 2001).

$$\xi = \frac{\omega_r^2 - \omega^2}{2\omega\omega_r} \frac{\operatorname{Re}[Y(\omega)]}{\operatorname{Im}[Y(\omega)]} \quad (7)$$

Using the values of the damping coefficient, the damping ratio and the natural frequency, the modal mass and the stiffness values can be obtained by Eqs. (8) and (9) (He and Fu 2001).

$$m = \frac{c}{2\xi\omega} \quad (8)$$

$$k = \omega^2 m \quad (9)$$



Fig. 6 An Exodermic deck suspended by two springs and ringed ropes



Fig. 7 Exciting the Exodermic deck by the impact hammer

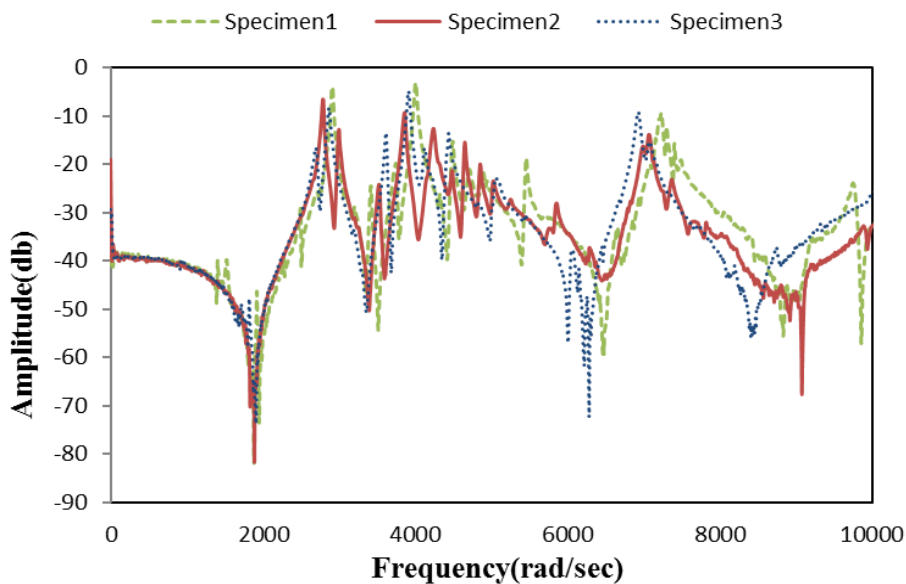


Fig. 8 Accelerance FRF of decks for excited point 1

To evaluate the frequency response function (FRF) of the decks, the structure should be excited by a specific force that is provided by means of an impact hammer or a shaker. In this research the decks were excited by an impact hammer (AU01, made by the APTECH Company) with 230 gr of weight. The response of the structure was recorded by an accelerometer (A/120/V made by the DJB Company) with negligible weight of 18 gr. The static load is applied to deck specimens by using a load-cell with 100 tons of capacity.

In order to obtain the dynamic properties of the Exodermic decks, modal analysis is conducted on decks. The decks are suspended as shown in Fig. 6 with two springs and two ringed ropes to reduce the effect of supports.

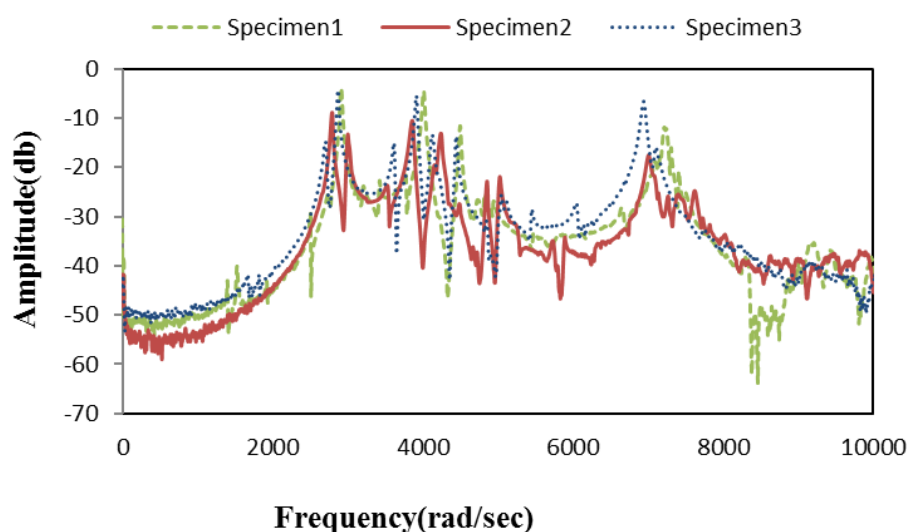


Fig. 9 Accelerance FRF of decks for excited point 2

After suspending the decks, an impact hammer is used to excite two points on the deck. The excited points (point 1 and point 2) are shown in Fig. 7. In order to enhance the accuracy of the method, the average response of five impacts was obtained and used in each point. Also the accelerometer was installed on the point 1 in all exciting.

The accelerance FRF data was recorded by a data logger in form of the complex numbers and then the recorded data was processed in a statistical program and eventually the FRF was plotted. In FRF plots the horizontal frequency axis is in linear scale and the vertical amplitude axis is in dB scale. FRF plots for excited points 1 and 2 are presented in Figs. 8 and 9, respectively.

To evaluate the damping ratio the peak picking or the Nyquist circle fit methods could be employed. If peak picking method is utilized, the ω_r , ω_1 and ω_2 frequencies should be extracted from the FRF plot. By substitution these frequencies into Eq. (2) the damping ratio would be obtained.

For the structure considered in this study, three modes which have the maximum amplitude among the resonance points, as shown in Figs. 8 and 9, were used in peak picking method and the results are presented in Table 4. The results given in Table 4 are the average damping ratios which were obtained from data related to the points 1 and 2 had been illustrated in Fig. 7.

Table 4 Natural frequency and damping ratio of the decks by using peak picking method

Deck NO.	Average frequency(rad/sec)			Average damping ratio(ξ) %		
	Mod1	Mod2	Mod3	Mod1	Mod2	Mod3
1	2910	4010	7115	0.44	0.44	0.48
2	2790	3860	7035	0.54	0.58	0.50
3	2870	3910	6965	0.58	0.44	0.44
Average	2856.67	3926.67	7038.33	0.52	0.49	0.47

The results show that the damping ratio is about 0.5%. The low value obtained for the damping ratio can be attributed to no energy depreciation by means of joints' wobbling or cracks' extending in the structure and so on, which are usually the main mechanisms of energy dissipation. Considering existing peaks which are near to each other, it is expected that the peak picking method may not lead to sufficiently accurate results. Therefore, to enhance accuracy, the Nyquist circle fit method is employed.

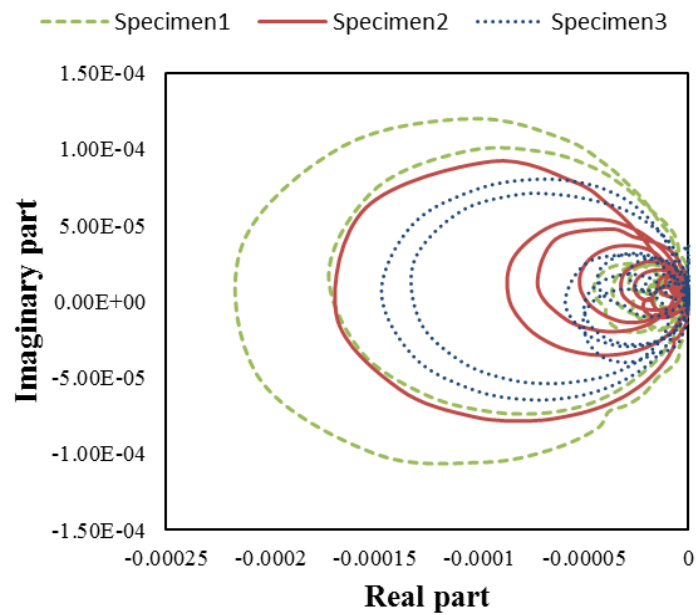


Fig. 10 Nyquist plot for mobility FRF of decks for excited point 1

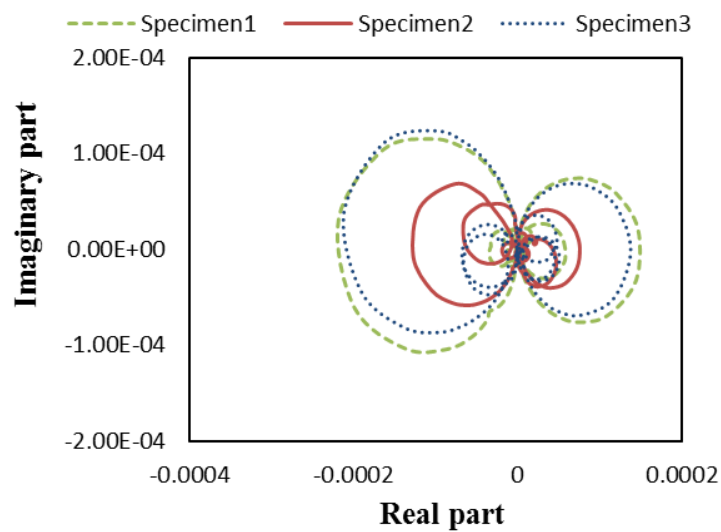


Fig. 11 Nyquist plot for mobility FRF of decks for excited point 2

Among the Nyquist plots for receptance, mobility and accelerance FRFs mere the Nyquist for mobility FRF is the real one. Thus, in order to plot the Nyquist circle the mobility FRF is required. Nonetheless what recorded by the data logger is the accelerance FRF. As the acceleration is the first derivative of the velocity to time, therefore in an attempt to reach the mobility FRF, accelerance FRF should be divided by $j\omega$. Having obtained the mobility FRF, and subsequently plotting its real part versus its imaginary part, the mobility Nyquist circles are plotted and presented in Figs. 10 and 11.

In these figures each circle refers to a vibrational mode, and its diameter would give the corresponding damping coefficient. In order to compute the damping ratios Eq. (7) could be used. Considering the diameter of the Nyquist circles, damping coefficients and damping ratios are given in Table 5.

Regarding Tables 4 and 5, damping ratio for the first mode is higher compared to the others, and consequently this mode is the most effective mode. By obtaining the values of c , ξ and ω , and using Eqs. (8) and (9), the modal mass and the stiffness values were evaluated and the results are given in Table 6.

As shown previously, the values obtained by the Nyquist circle fit method are in good agreement with those obtained from the peak picking method, and the maximum damping ratio is related to the first mode.

In order to verify the obtained results, Abaqus finite-element software was employed to investigate the dynamic behavior of an Exodermic deck with the same dimensions used in the experimental program in the free support condition.

The properties of modeling materials were adopted as same as the attributes of materials which were used in the laboratory. Rebar, main bearing bar, distribution bar and concrete members were modeled as truss, shell, shell, and solid sections, respectively. Rebar and main bar members were embedded into the concrete member and the shell-to-solid constraint was applied between the distribution members and the concrete member. The T3D3, S8R and C3D20R element types were

Table 5 Natural frequency, coefficient and damping ratios of the decks by using Nyquist circle plot method

Deck NO.	Average damping coefficient (c)			Average frequency (rad/sec)			Average damping ratio (ξ) %		
	Mod3	Mod2	Mod3	Mod2	Mod3	Mod2	Mod3	Mod2	Mod1
1	25000	6369.85	25000	6369.85	25000	6369.85	0.55	0.45	0.50
2	14695	12494.5	14695	12494.5	14695	12494.5	0.56	0.54	0.66
3	16949.15	7016.10	16949.15	7016.10	16949.15	7016.10	0.48	0.66	0.67
Average	18881.34	8626.82	18881.34	8626.82	18881.34	8626.82	0.53	0.55	0.61

Table 6 Modal mass and stiffness of the decks

Deck NO.	Average frequency(rad/sec)			Average damping ratio(ξ) %		
	Mod1	Mod2	Mod3	Mod1	Mod2	Mod3
1	16411613636	2833917955	1346544992	314.73	176.76	158.97
2	9194215402	4453664525	1457466536	187.24	300.52	187.46
3	12256000986	2077855222	1317780898	254.33	135.97	160.74
Average	12620610008	3121812567	1373930809	252.10	204.42	169.06

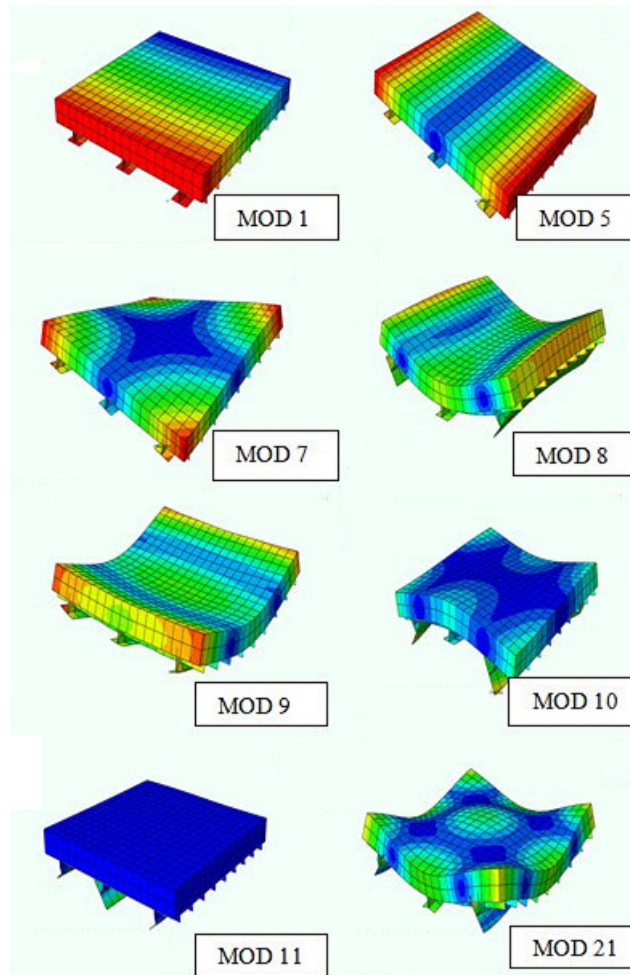


Fig. 12 Some mode shapes which were obtained via finite-element method

applied for truss, shell, and solid sections, respectively. The results for the mode shapes are shown in Fig. 12.

The natural frequencies for various mode shapes are also given in Table 7. According to the values of Table 7, for the four initial modes, the frequencies are very small comparatively. Therefore, these modes are rigid translation motion modes. The next two mode shapes have higher frequencies without bending behavior indicating rigid rotational motion modes around a horizontal axis. From 7th mode onwards, the strain contour shows bending and rotation in relation to different axes. Furthermore, the frequencies are enough large; as a result, these modes are considered as flexural (bending and torsion) modes.

In addition, the frequencies of the 8th, 10th and 21st rows in Table 7 and the experimental results presented in Tables 4 to 6 have small differences. For instance, the error percentage for these frequencies (modes 1, 2 and 3) are 0.0011, 0.006 and 0.02, respectively. Based on the values of Table 7, Figs. 8 and 9, an acceptable accordance could be found between the results of the

Table 7 Frequencies computed by using finite-element method

Mode No.	Frequency (rad/s) for mix.1
1	0
2	11.44 E-04
3	17.02 E-04
4	21.55 E-04
5	312.56
6	386.09
7	1601.53
8	2886.10
9	3583.43
10	3901.01
11	4118.17
12	4213.69
13	4231.46
14	4440.15
15	4503.58
16	4605.25
17	4625.35
18	5549.20
19	5564.77
20	5588.51
21	7192.48
22	7768.36
23	8064.78
24	8155.84
25	8164.00

frequencies obtained by finite element method and those obtained experimentally. It is worth mentioning that some mode shapes (e.g. the mode shape located in the 7th row of Table 7) did not appear in experimental results. This is due to using a rope for hanging the deck acted as a weak restraint.

4. Static evaluation

The casted decks were placed on the hinged support in order to load forces carried out by means of a 100 ton load-cell. The load is applied through a plate with 300 × 300 mm of dimensions and 30 mm of thickness at the center of the decks. To provide the required stiffness between the load-cell and the surface of the decks some rigid parts were used as shown in Fig. 13.

A strain-gauge with the length of 40 mm which was located 50 mm far from the plate in transverse direction (Perpendicular to axis of support) was used to record the concrete strain.



Fig. 13 Rigid parts used in order to provide stiffness between load-cell and the deck

Also a strain-gauge which was located at the center of each main bar in transverse direction was used to record the strain of main bar's flange.

Two deck specimens were tested under the static load (positive bending) with load step of 40 kN per cycle and finally the decks failure occurred at the load of 350 KN due to punching in concrete part as shown in Fig. 14. In fact the applied load is higher than the concrete shear capacity.



Fig. 14 Failure mode of the decks under positive bending

The force-strain curves of the concrete slab, the steel main bars, and the force-displacement curves at the center of the decks are presented in Figs. 15 to 17.

According to Fig. 15 and 16 the strains increase linearly for both concrete and steel parts to reach the maximum value of 350 KN, afterwards the load was dropped due to punching in the concrete slab. As shown in Fig. 17, the maximum vertical displacement of the decks under service load of 80 KN is about 2 mm that can be controlled by increasing height of T-shaped sections.

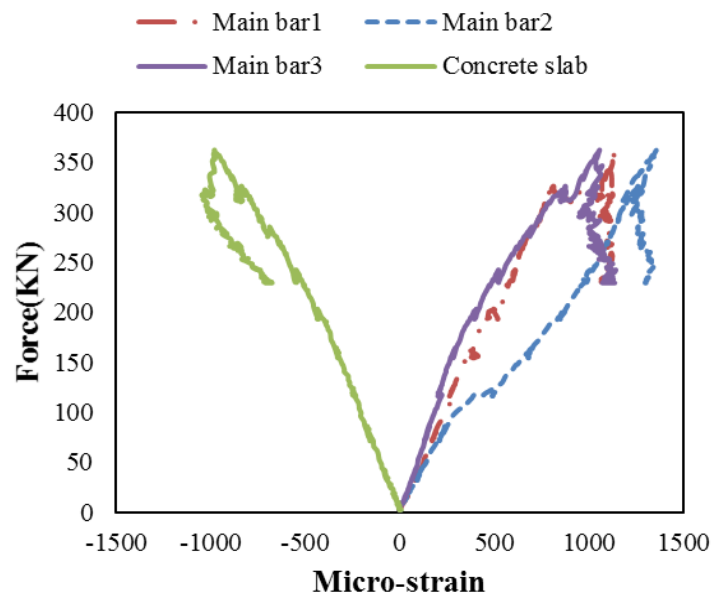


Fig. 15 Force-strain curve for specimen 1

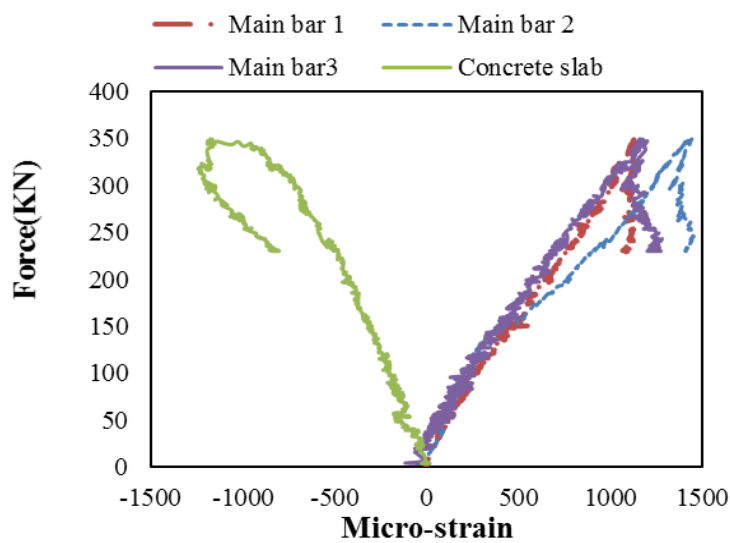


Fig. 16 Force-strain curve for specimen 2

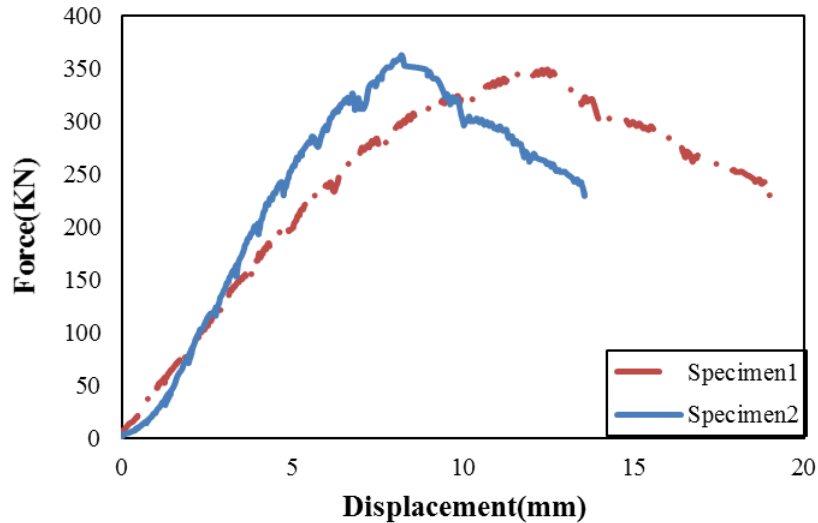


Fig. 17 Force-displacement curve



Fig. 18 An Exodermic deck under negative bending

Since the deck is used in form of continuous spans, its behavior under negative bending conditions is important. To examine this point, an Exodermic deck was placed on the restrains in reverse configuration as shown in Fig. 18.

Formation of crack patterns, strain of the main bars and concrete slab are shown in Fig. 19 and Fig. 20. Due to formation of cracks under the strain-gauge, the strain of concrete was not recorded over 50 KN of load.

As shown in Fig. 19, strains increase linearly and finally the deck fails at 180 KN of load. This shows that the negative bending capacity of the deck is about 50% of its capacity under positive bending. As shown in Fig. 20, due to the transition of the load through distribution bars, cracks were extended to all directions that confirm the plate behavior of the deck. The failure mode of the decks under positive bending was punching shear. According to ACI 318 (2005), the shear capacity of the concrete could be determined by Eq. (10)

$$V_c = \min\left(\frac{\sqrt{f'_c}}{3}bd, \left(1 + \frac{2}{\beta}\right)\frac{\sqrt{f'_c}}{6}bd, \left(\frac{\alpha_s d}{b} + 2\right)\frac{\sqrt{f'_c}}{6}bd\right) \quad (10)$$

Concrete shear capacity obtained from Eq. (10) is 334.57, which has an appropriate accordance with the experimental results.

Finally, in order to compare the weight of the Exodermic deck with the weight of equivalent ordinary reinforced concrete slab (ORCS), an ORCS was designed according to ACI 318 (2005)

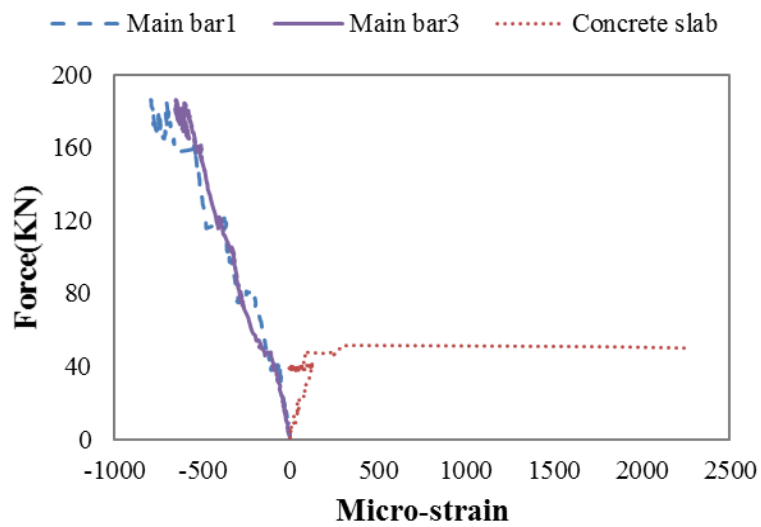


Fig. 19 Force-strain curve for specimen under negative bending



Fig. 20 Cracks formation on the deck, under negative bending

Table 8 Design parameters for equivalent ordinary reinforced concrete slab

	M_d (N.m)	M_n (N.m)	ρ	ρ'	ρ_b	$\bar{\rho}_b$	$\bar{\rho}_{min}$
Positive bending	81616.50	81618.77	0.0053	0.0025	0.0478	0.0501	0.1060
Negative bending	41882.85	53531.07	0.0025	0.0053	0.0478	0.0526	0.1110

for the 81616500 N.m positive bending moment, 418828850 N.m negative bending moment, and 362 KN shear force. In this regard, the thickness of the ORCS was considered as 298 mm, and subsequently the design parameters are given in Table 8.

Where M_d , M_n , ρ , ρ' , ρ_b , $\bar{\rho}_b$, $\bar{\rho}_{min}$ are: design moment, nominal moment, tension reinforcement ratio, compression reinforcement ratio, balanced reinforcement ratio without compression reinforcement, balanced reinforcement ratio and minimum tension reinforcement on compression reinforcement yielding boundary, respectively. By comparing the designed ORCS with the Exodermic deck, it can be deduced that the weight of the Exodermic deck is about 40% of that of the ORCS.

5. Conclusions

In this study, an experimental program was conducted to investigate the mechanical properties of Exodermic steel-concrete composite decks with perfobond shear connectors. In order to evaluate the dynamic properties of the Exodermic decks, a modal analysis using the frequency response function method was employed. Natural frequencies, damping ratios as well as some physical properties such as the stiffness and the modal mass were obtained. Static loading test was conducted on constructed Exodermic decks with perfobond shear connectors to yield the strengths of decks under a concentrated loading. Final results gave rise to following conclusions.

- Failure of the decks under positive bending was punching-shear and the bending capacity of the decks under negative bending was about 50 percent of their capacity under positive bending.
- The results show that the first four modes are the rigid translational motion modes and the next two modes seem to be rigid rotational motion modes around a horizontal axis and from the 7th mode to the end are flexible modes.
- The experimental results show that the first mode is the most effective mode among the obtained modes.
- The range of damping ratios was about 0.5% due to lack of energy depreciation by means of joints wobbling or cracks extending in the structure.
- Formation of cracks in longitudinal and transverse directions indicated that the behavior of the deck is similar to a plate.
- Weight of an Exodermic deck is about 40% of an equivalent ORCS designed according to ACI 318 (2005).

Acknowledgments

The authors would like to thank the staff of concrete technology laboratory of Babol Noshirvani University of Technology for their helpful assistances. Supports provided by Faculty of Civil Engineering in Babol Noshirvani University of Technology are also appreciated.

References

- ACI 318 (2005), *Building Code Requirements for Structural Concrete and Commentary*, MI, USA.
- ASTM C33 (2001), *Standard Specification for Concrete Aggregates*, American Society for Testing and Materials, PA, USA.
- Ciutina, A.L. and Stratan, A. (2008), "Cyclic performances of shear connectors", *Proceedings of the Composite Construction in Steel and Concrete Conference*, CO, USA, July.
- Gorkem, S.E. and Husem, M. (2013), "Ultimate behavior of composite beams with shallow I-sections", *Steel Compos. Struct., Int. J.*, **14**(5), 493-509.
- He, J. and Fu, Z.F. (2001), *Modal Analysis*, Butterworth-Heinemann, Oxford, UK.
- Higgins, C. and Mitchell, H. (2001), "Behavior of composite bridge decks with alternative shear connectors", *ASCE J. Bridge Eng.*, **6**(1) 17-22.
- Hou, Z.M., Xia, H. and Zhang, Y.L. (2012) "Dynamic analysis and shear connector damage identification of steel-concrete composite beams", *Steel Compos. Struct., Int. J.*, **13**(4), 493-509.
- Kim, H.Y. and Jeong, Y.J. (2009), "Steel-concrete composite bridge deck slab with profiled sheeting", *J. Construct. Steel Res.*, **65**(8-9), 1751-1762.
- Kim, H.Y. and Jeong, Y.J. (2010), "Ultimate strength of a steel-concrete composite bridge deck slab with profiled sheeting", *Eng. Struct.*, **32**(2), 534-546.
- Kim, S.H. and Choi, J.H. (2010), "Experimental study on shear connection in unfilled composite steel grid bridge deck", *J. Construct. Steel Res.*, **66**(11), 1339-1344.
- Leonhardt, E.F., Andra W., Andra H.P. and Harre W. (1987), "New improved shear connector with high fatigue strength for composite structures", *Beton-Und Stahlbetonbau*, **12**, 325-331.
- Macháček, J. and Studnicka, J. (2002), "Perforated shear connectors", *Steel Compos. Struct., Int. J.*, **2**(1), 51-66.
- Nishimura, A., Okumura, T. and Ariga, Y. (1971), "Shear connector utilizing the reinforcing steels in composite girder slab", *Proceedings of the Symposium on New Techniques in the Construction of Structures, 17th National Symposium on Bridge and Structural Engineering, Japan Society for the Promotion of Science*, Tokyo, Japan.
- Oguejiofor, E.C. and Hosain, M.U. (1992), "Behavior of perfobond rib shear connectors in composite beams: Full-size tests", *Canadian Journal of Civil Engineering*, **19**(2), 224-235.
- Oguejiofor, E.C. and Hosain, M.U. (1994), "Parametric study of perfobond rib shear connectors", *Can. J. Civil Eng.*, **21**(4), 614-625.
- Oguejiofor, E.C. and Hosain, M.U. (1996), "Numerical analysis of push-out specimens with Perfobond rib connectors", *Comp. Struct.*, **62**(4), 617-624.
- The D.S Brown Company (2007), "An Introduction to: Exodermic™ Bridge Decks" <http://www.exodermic.com/docs/pdf/brochure/ExoRev.pdf>
- Velanda, M.R. and Hosain, M.U. (1992), "Behavior of perfobond rib shear connectors: Push-out tests" *Can. J. Civil Eng.*, **19**(1), 1-10.
- Zellner, W. (1987), "Recent designs of composite bridges and a new type of shear connectors", *Proceedings of the IABSE/ASCE Engineering Foundation Conference on Composite Construction*, New England College, USA.